



ELSEVIER

Available online at www.sciencedirect.com

Geomorphology xx (2007) xxx–xxx

GEOMORPHOLOGY

www.elsevier.com/locate/geomorph

Qualitative landslide susceptibility assessment by multicriteria analysis: A case study from San Antonio del Sur, Guantánamo, Cuba

Enrique A. Castellanos Abella^{a,*}, Cees J. Van Westen^{b,1}

^a Instituto de Geología y Paleontología (IGP), Vía blanca y Carretera Central, San Miguel del Padrón, CP 11000, Ciudad de La Habana, Cuba

^b International Institute for Geoinformation Science and Earth Observation (ITC), ITC, PO, Box 6, 7500 AA Enschede, The Netherlands

Received 28 January 2005; received in revised form 27 January 2006; accepted 16 October 2006

Abstract

Geomorphological information can be combined with decision-support tools to assess landslide hazard and risk. A heuristic model was applied to a rural municipality in eastern Cuba. The study is based on a terrain mapping units (TMU) map, generated at 1:50,000 scale by interpretation of aerial photos, satellite images and field data. Information describing 603 terrain units was collected in a database. Landslide areas were mapped in detail to classify the different failure types and parts. Three major landslide regions are recognized in the study area: coastal hills with rockfalls, shallow debris flows and old rotational rockslides denudational slopes in limestone, with very large deep-seated rockslides related to tectonic activity and the Sierra de Caujerí scarp, with large rockslides. The Caujerí scarp presents the highest hazard, with recent landslides and various signs of active processes. The different landforms and the causative factors for landslides were analyzed and used to develop the heuristic model. The model is based on weights assigned by expert judgment and organized in a number of components such as slope angle, internal relief, slope shape, geological formation, active faults, distance to drainage, distance to springs, geomorphological subunits and existing landslide zones. From these variables a hierarchical heuristic model was applied in which three levels of weights were designed for classes, variables, and criteria. The model combines all weights into a single hazard value for each pixel of the landslide hazard map. The hazard map was then divided by two scales, one with three classes for disaster managers and one with 10 detailed hazard classes for technical staff. The range of weight values and the number of existing landslides is registered for each class. The resulting increasing landslide density with higher hazard classes indicates that the output map is reliable. The landslide hazard map was used in combination with existing information on buildings and infrastructure to prepare a qualitative risk map. The complete lack of historical landslide information and geotechnical data precludes the development of quantitative deterministic or probabilistic models.

© 2007 Elsevier B.V. All rights reserved.

Keywords: Landslide susceptibility; Geomorphological mapping; Heuristic analysis; Multicriteria analysis

1. Introduction

As in most developing countries, landslide inventory maps are still scarce in Cuba, due to the limited resources available for research. Most conventional landslide studies in Cuba are descriptive, and a few focus on hazard assessment. Moreover, most of the quantitative

* Corresponding author. Tel.: +53 7 55 7232; fax: +53 7 55 7004.

E-mail addresses: castellanos@itc.nl (E.A. Castellanos Abella), westen@itc.nl (C.J. Van Westen).

¹ Tel.: +31 53 4874 444; fax: +31 53 4874 400.

risk assessment methods that have been developed elsewhere are case-specific and require many types of data, on landslide occurrence and impact, most of which are not yet available in Cuba.

There are four different approaches to the assessment of landslide hazard: landslide inventory-based probabilistic, heuristic (which can be direct geomorphological mapping, or indirect qualitative map combination), statistical (bivariate or multivariate statistics) and deterministic (Soeters and Van Westen, 1996; Aleotti and Chowdhury, 1999; Guzzetti et al., 1999). Landslide risk-assessment methods are classified into three groups, as qualitative (probability and losses in qualitative terms), semi-quantitative (indicative probability, qualitative terms) and quantitative (probability and losses both numerical) (Lee and Jones, 2004).

The heuristic approach is considered to be useful for obtaining qualitative landslide hazard maps for large areas in a relatively short time. It does not require the collection of geotechnical data, although detailed geomorphological mapping is essential. The heuristic approach may result in more reliable susceptibility maps than using statistical methods, where a considerable amount of generalization always needs to be accepted in the analysis. This is particularly relevant in Cuba, where the geomorphological setting exhibits high spatial variability. Qualitative risk assessment procedures in many countries are heuristic, e.g. in Switzerland (Lateltin, 1997). The qualitative approach is based on expert opinion and the risk areas are categorized by such terms as “very high”, “high”, “moderate”, “low” and “very low”. The increasing popularity of geographic information systems (GIS) has led to many studies, mainly using indirect susceptibility-mapping approaches (Aleotti and Chowdhury, 1999). As a consequence fewer investigations use GIS in combination with a heuristic approach, either geomorphological mapping, or index overlay mapping (e.g. Barredo et al., 2000; Van Westen et al., 2000, 2003).

Nowadays, new decision-support tools are available for GIS-based heuristic analysis. They allow better structuring of various components, including both objective and subjective aspects and compare them in a logical and thorough way (Saaty, 1980). Decision-support tools such as (spatial) multicriteria analysis have not been popular for qualitative assessment of landslide hazard.

This research combines geomorphological information with GIS-based decision-support tools to develop a heuristic landslide-hazard assessment model in San Antonio del Sur, Guantánamo, Cuba at 1:50,000 scale.

2. The study area

The study area, within the San Antonio del Sur municipality, is located in eastern Cuba (Fig. 1) 60 km from the city of Guantánamo, the capital of the province with the same name. The main access to the area is by the coastal road connecting Guantánamo and the eastern municipalities.

The geology and tectonic setting of the eastern part of Cuba is rather complicated, and includes several geological and tectonic environments in a relatively small area. The different tectonic and structural processes have overlapped over geological time in such a way that it is difficult to separate them spatially and temporally. Moreover, the area remains an active tectonic zone on the northern boundary between the Caribbean and North American plates, as evidenced by many neotectonic features and by the continuous general uplift of the area. The general geology of Cuba is divided into two principal units: a foldbelt and a neoautochthon (Iturralde-Vinent, 1996), which unconformably overlies the foldbelt (Fig. 1). The eastern part of Cuba and the study area have been studied by Nuñez et al. (1981), Nagy et al. (1983), Millán and Somin (1985) and Franco (1992).

The San Antonio del Sur area contains geological units from both the foldbelt and the neoautochthon. The foldbelt consists of a Northern Ophiolite belt, a Cretaceous Volcanic arc, a Paleocene Middle Eocene volcanic arc and a Late Middle Eocene piggyback basin (Fig. 1). The ophiolites are represented in the study area by a hilly zone in the southeast called “Sierra del Convento” (Fig. 2). It is the surface expression of a larger body considered as a relic of the basement, which emerged due to spreading of the oceanic crust, pushed from the south by tectonic events (Chang and Suarez, 1998). Rocks of the Cretaceous volcanic arc belonging to the Sierra del Purial Formation underlie the eastern part of the study area with low grade and high pressure metamorphism. Deposits from the Paleocene volcanic arc, belonging to the El Cobre Group, can be found in the north of the area (Fig. 1). The piggyback basin corresponds to the Paleocene–middle Eocene volcanic arc. The Charco Redondo, San Ignacio and San Luis formations represent this basin in the study area. These formations cover the northeast up to the central part, and consist of polymictic sandstones, mudstones, marls, clays, limestone clays, bioclastic limestone, sandy limestone and polymictic conglomerates.

The western and central part of the study area is underlain by the “Neoautochthon”, recent units formed in situ, and which are represented in the study area by formations from three transgression–regression phases which occurred since the Late Eocene (Iturralde-Vinent,

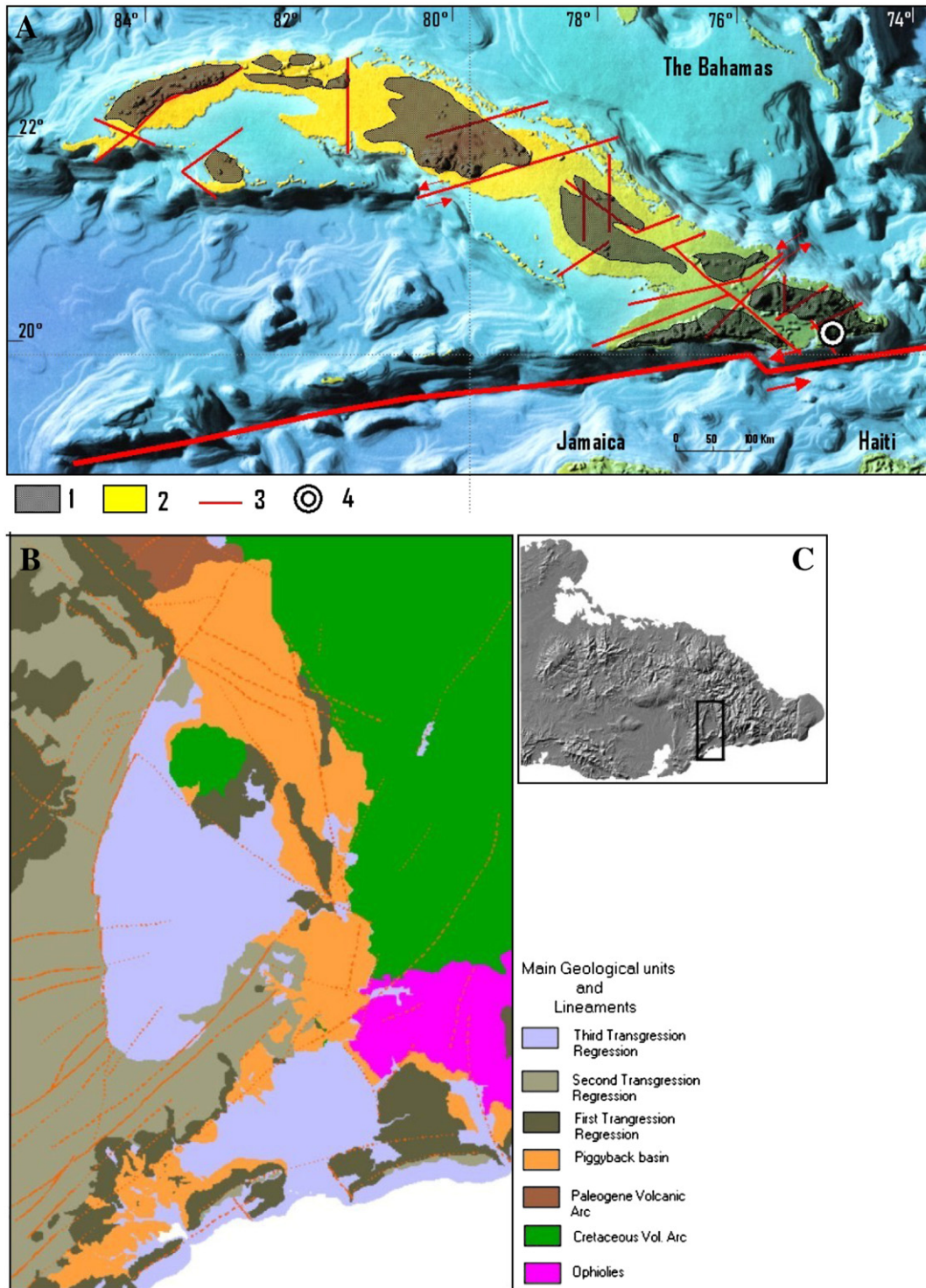


Fig. 1. A: Location of study area in Cuba. 1 = outcrops of the foldbelt, 2 = Eocene to Recent neo-autochthonous deposits, 3 = Main faults, 4 = Study area. B: general geological map of the San Antonio del Sur municipality, Guantánamo province, Cuba. C: Shaded relief of Eastern Cuba with study area outlined. North is up and the area is 20 by 30 km.

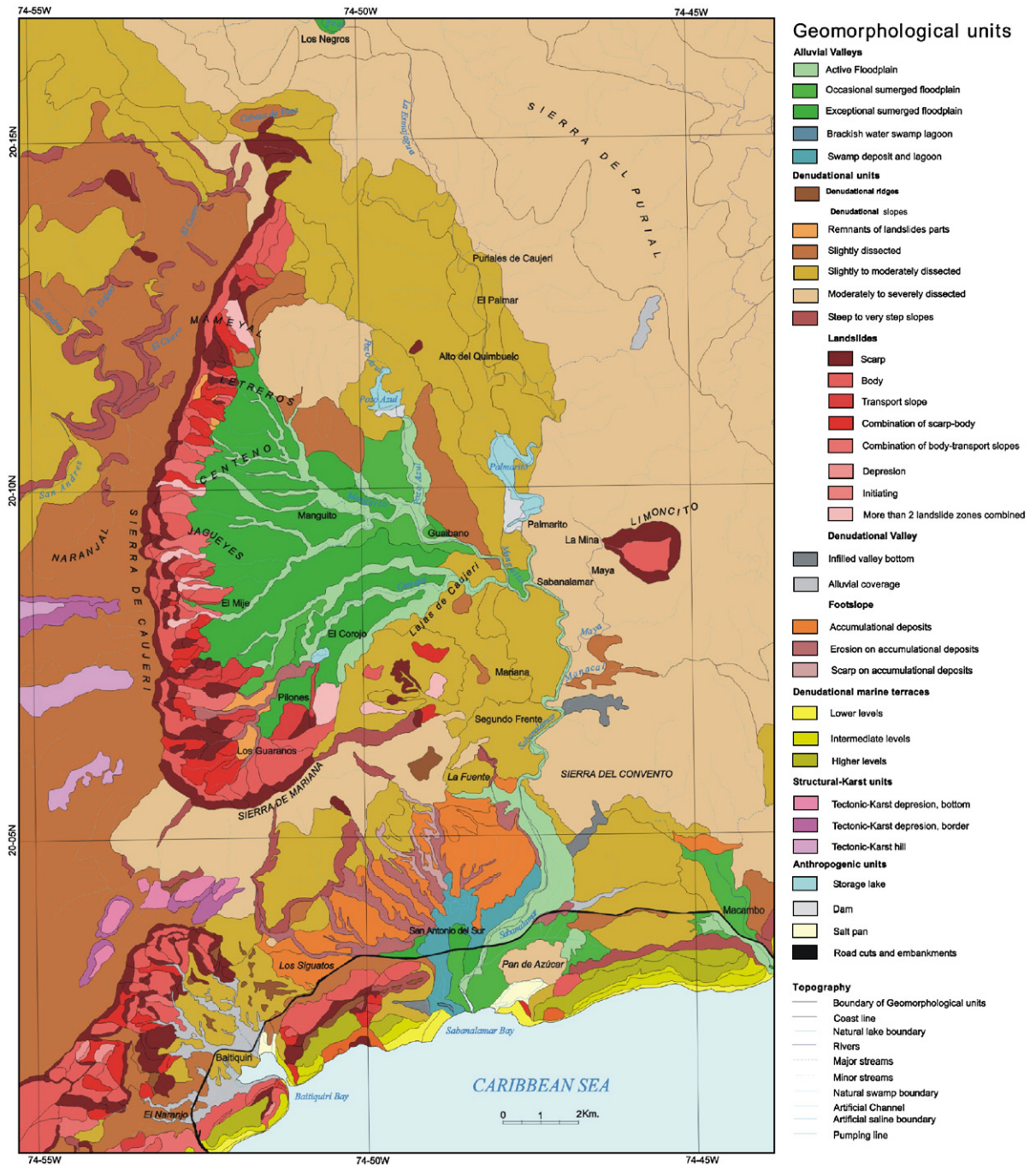


Fig. 2. Geomorphological map. San Antonio del Sur, Guantánamo Province, Cuba.

1996). The first such cycle is from Late Eocene to Oligocene (Phase1) and consists of alternating layers of sandstone, mudstone and calcareous clay. The second cycle is from Early Oligocene–Late Miocene (Phase2), and is characterized by alternating layers of clastic, bioclastic and biogenic limestone (Fig. 1B). The third cycle is Late Pliocene to recent (Phase3) and is

characterized by algae-bearing bioherm limestones, with corals, and recent marine sediments.

3. Geomorphology and landslide occurrence

The geomorphology of the study area is conditioned by the Caribbean–North American inter-Plate zone, and

the paleoclimatic oscillations during the Quaternary period. Fig. 3 presents an overview of the study area as an anaglyph image, generated from a digital elevation model and a SPOT-PAN image. For 3-D viewing of the

image, red–green glasses are required. The inter-Plate boundary consists of a strike–slip fault system (Fig. 1) of which secondary faults have topographic effects inland (see Fig. 3, complexes C and B). The Quaternary

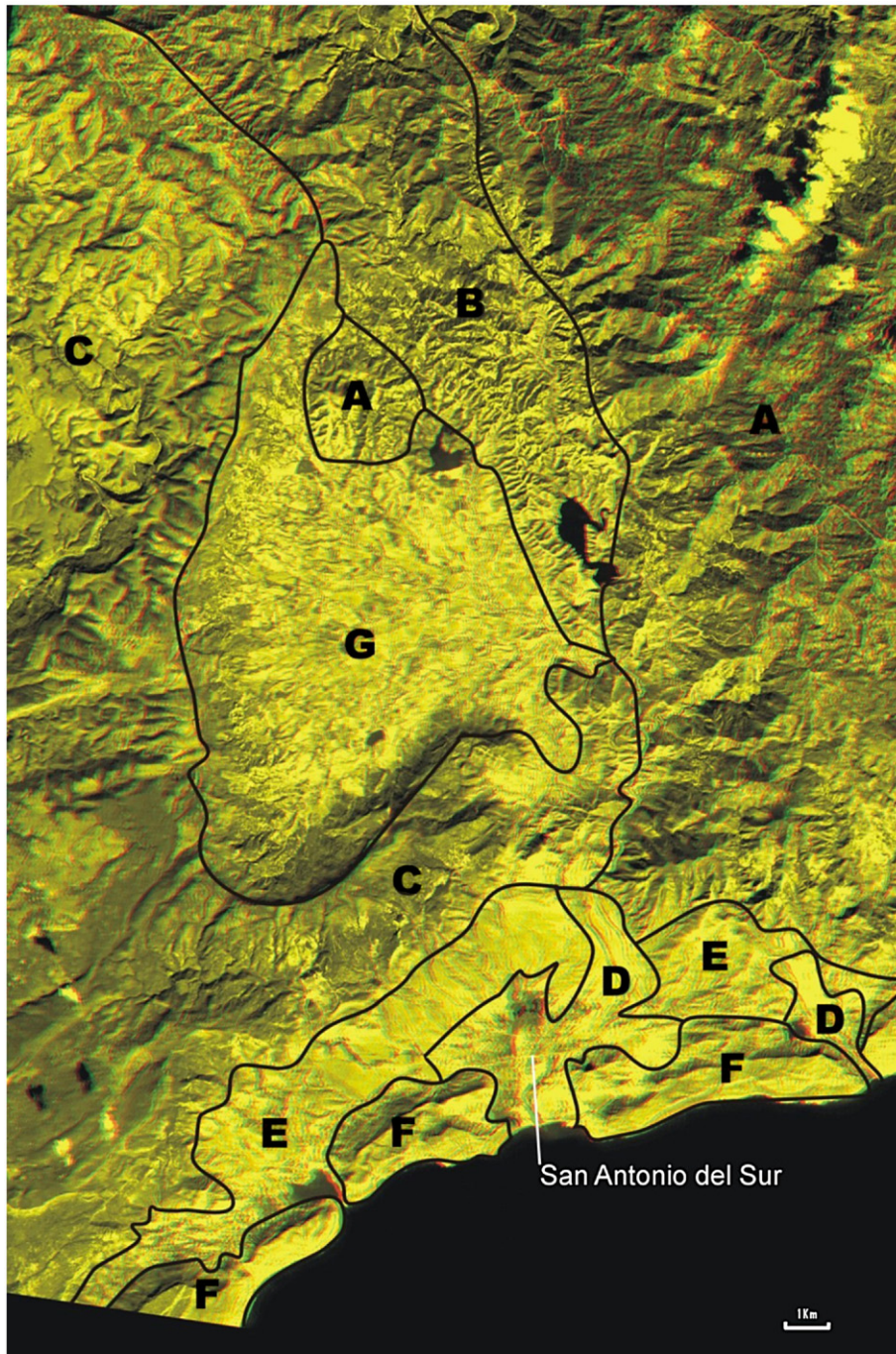


Fig. 3. Geomorphic complexes of the study area: A, B, C: denudational hills in metamorphic rocks, terrigenous rocks, and in limestone respectively; D: Alluvial units; E: Accumulative slopes; F: Coastal hills; G: Puriales de Caujeri depression. This anaglyph image requires red–green glasses for viewing in 3-D.

sea-level oscillations left coastal hills with marine terraces and abandoned valleys (see Fig. 3, complexes D, E and F).

A geomorphological map, including the landslide inventory, (Fig. 2) at a scale of 1:50,000 was prepared from interpretation of two sets of aerial photographs (of 1:25,000 and 1:37,000 scale) and fieldwork. Both photo sets correspond to a national aerial survey carried out at the beginning of the 1970s. The 1:37,000 scale photos (55 in total) cover the whole study area with four flight lines and were taken between 2-Feb-1972 and 19-Mar-1972. The 1:25,000 scale photos (46 in total) cover the south-west part of the study area in three flight lines and were taken between 5-Dec-1971 and 21-Dec-1971. The photos were interpreted with a TOPCON stereoscope on transparent paper and transferred to digital format by on-screen digitizing using other image products for double checking (anaglyph, shaded DEM, Landsat TM true color composite and digital topographic map). The photo-interpreted units were checked in the field by three people during a fieldwork campaign which took three weeks.

The area was divided into 603 terrain mapping units (TMU). A TMU can be considered a homogeneous mapping unit on the basis of geomorphologic origin, physiography, lithology, morphometry, and soil geography (Meijerink, 1988). Normally, a single landslide was considered an individual TMU. In certain cases, when the size was large enough, landslide zones such as scarps, bodies and depressions were also considered as separate TMUs. The units have been combined into the following geomorphological complexes:

- Denudational hills (metamorphic rocks, terrigenous rocks, and limestone) (A, B and C in Fig. 3)
- Alluvial units and accumulative slopes (D and E in Fig. 3)
- Coastal hills (F in Fig. 3)
- Puriales de Caujeri depression (G in Fig. 3)

3.1. Denudational hills

Denudational hills can be separated by the underlying lithology into a limestone plateau (C in Fig. 3), metamorphic hills (A in Fig. 3) and terrigenous hills (B in Fig. 3). The plateau is a monocline at an average altitude of 500 m, composed mainly of limestone from the Yateras formation (Phase2) with extensive karst processes and additional erosion where the underlying mudstone and calcareous clay from the Maquey formation (Phase3), are exposed. The area is dominated by neotectonic processes such as faulting, and a number of

large deep-seated mass movements are observed which could reflect a mix of gravitational and tectonic movements (Fig. 3). The landslides are concentrated in the north part of Baitiquiri and El Naranjo. As the area is strongly affected by active faults the landslides are located in three main “steps” from the limestone hills toward the coast. In the upper part the landslides occur in limestone rocks of Yateras formation (Fig. 2). In the next two steps the landslides occur over terrigenous materials (Fig. 1). All the main landslide features are aligned with the major faults in the directions SW–NE, N–S and W–E, and they occur often where the faults are converging. In some of the upper portions of the large landslide masses the total amount of displacement has not been more than a few meters. Displacements were greater on the lower steps and individual landslides are more difficult to delimit because they occurred in a multiple and successive way, often one on top of another. The main types in this area are rotational rockslides in the upper part, often with multiple scarps and debris slides in the lower parts, combined with extensive rill and gully erosion. It is difficult to define the age of the landslides, but the multiple and complex landslide forms indicate that mass movements have been active over a long period, associated with the activity of the faults, and probably with relatively minor individual displacements per event. The most recently known landslide occurred in 1997, during an intensive rainy season, but probably was caused by a leaking water pipe; it destroyed a mini-hydroelectric power plant.

Landslides in the denudational hills underlain by metamorphic and terrigenous rocks (Fig. 3, A and B) are generally smaller than those in the limestone hills, and are not so related to tectonic lineaments. Most of them are shallow rotational landslides occurring rather at random on the steep hill-slopes or along river incisions.

3.2. Alluvial units and accumulative slopes

The Alluvial valley complex is related to the recent sediments accumulated by to the principal river systems (Figs. 3D and 2 for names). Sabanalamar river floodplain, Macambo river floodplain and the most recent fluvial channels in the Caujeri valley are part of this complex. They are composed of alluvial and swampy deltaic deposits where the rivers end in submerged valleys, due to tectonic uplift. This complex is essentially a fluvial plain with a combination of erosive and accumulation processes. Accumulation prevails in the Sabanalamar and Macambo floodplains and erosion in the Caujeri valley. Three floodplain levels are recognizable: active, occasionally

submerged and exceptionally submerged floodplains. The area is regularly inundated during intensive rain. Close to Sabanalamar Bay and in the surroundings of San Antonio del Sur town, there are brackish water lagoons and swamps. Mangrove vegetation is abundant only in the mouth of the Sabanalamar River.

The accumulational slopes are located in the northern part of the coastal hills (Fig. 3). It is an intra-mountainous fluvio-marine deltaic plain approximately 2 km wide. Slopes slightly to the south (sea) side at 5 to 15°. The materials range from colluvial, close to the mountains, to fluvio-marine. This complex seems to belong to an old planation surface, which collected all the sediments coming from the upward area, what is now Sierra de Mariana (Fig. 2), during the Pleistocene. The extension and volume of the Quaternary sediments reveals that rainfall at that time was higher than currently. This might be true considering the fact that in the northern border of the Sierra de Mariana the drainage seems to be cut-off due to large mass movements. In both the western and eastern sides of the area, the Pleistocene sediments are not present. In the western side the drainage system was sufficiently strong to erode the sediments to the Baitiquirí Bay, besides this part appears to be slightly more uplifted. In the eastern part the pre-Quaternary formation overlies the ophiolites and the area has an irregular relief. The planation surface is raised 10 to 30 m above the current erosion levels, and around ten new channels have eroded the old plain and generated erosional scarps with the same height differences. The alluvial unit and accumulational slopes do not contain any major landslide features.

3.3. Coastal hills

These hills parallel the coastline (Fig. 3), with variable length and a width between 1 and 2 km. Three coastal hills can be differentiated, between El Naranjo and Baitiquirí Bay, between the Baitiquirí bay and Sabanalamar Bay (Loma Los Aposentos) and between Sabanalamar Bay and Macambo town (see names in Fig. 2 and relief in Fig. 3 F). The north side is totally covered by the Maquey formation (Phase1), mudstone and calcareous clay susceptible to landslides. The coastal slope, characterized by marine terraces is composed of the Maya formation (Phase3) consisting of recent (Holocene) marine deposits. These deposits act as “rings” of the coastal hills and are uplifted between 5 and 10 m from current sea level.

The different material and morphological characteristics on both sides of the coastal hills also result in different landslide types. Northern slopes are characterized by frequent, but small debris flows. On the coastal

side, rockfalls occur in the marine terraces, caused by a combination of karstic dissolution and physical weathering processes and triggered by wave erosion. Large blocks with volumes between 15 to 40 m³ can be found as part of the rockfalls. On top of the cliff various cracks delimit the boundaries of future rockfall events. Magaz et al. (1991) mapped three large rotational and two translational rockslides in the marine terraces, covering the entire seaward side of the coastal hills. Two of the large rotational landslides are pre-Holocene because the lower terrace was formed on top of the landslide toe. The third landslide in Los Aposentos coastal hill (Fig. 4A and B) is more recent than the others are since the lower terrace (Holocene) was also destroyed.

3.4. Puriales de Caujerí depression

By far the most striking geomorphological feature in the study area is the large oval shaped depression (Puriales de Caujerí valley), which is considered to be a graben with elevation differences up to 500 m. The valley is limited on the west by a large scarp of the Sierra de Caujerí, with some active retrogressive mass movements. On the southern and northern parts the valley is also surrounded by major fault scarps. The origin of the Puriales de Caujerí depression can be interpreted as a combination of tectonic and mass wasting processes. The main fault systems (Sierra de Mariana and Sierra de Caujerí) started to generate a graben depression after the second Transgression–Regression period (Lower Miocene to Late Miocene). After that, the 15-kilometer-long N–S oriented Sierra de Caujerí carp, 300 to 400 m high, has been the main area of landslide activity. In the north the scarp ends 3 to 5 km north of Mameyal and has less recent landslide activity. In the south the scarp intersects the fault-controlled Sierra de Mariana scarp creating another area with large landslides. Fig. 4 (C, D and E) shows some of the landslides in the Caujerí scarp.

The most catastrophic landslide in the Sierra de Caujerí scarp occurred after three days of heavy rain during the passing of cyclone Flora on October 8, 1963, the most devastating meteorological event known that affected Cuba (see Fig. 4 D and E). A total of 1100 mm of rainfall in three days was recorded in the Sierra de Caujerí area (Trusov, 1989). The successive rotational rockslide occurred in two pulses at about 45 min intervals, which allowed some of the inhabitants to escape, whereas 5–10 others were killed. No technical report was made directly after the event although some data were recorded during the fieldwork when a number of interviews were held with some of the survivors. However, due to the long time since the occurrence of

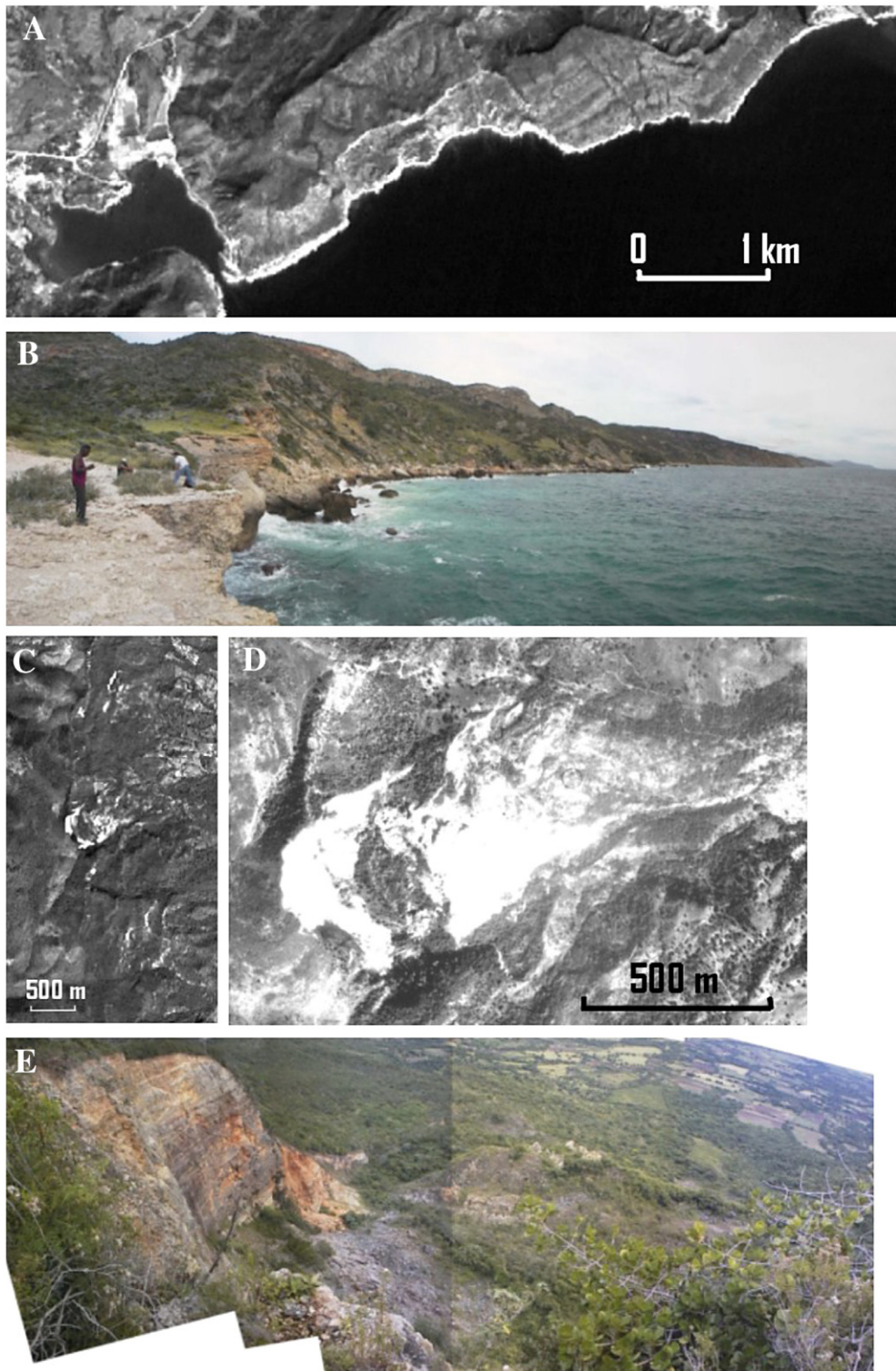


Fig. 4. Different landslides from the study area. A (Spot Pan 28/12/1994) and B: Los Aposentos landslide, typical rotational landslide in the coastal hills; C (Spot Pan 28/12/1994), D (Aerial photo K10 survey, 02/02/1972), E: Jagueyes landslide, large landslide movements in the Sierra de Caujeri scarp.

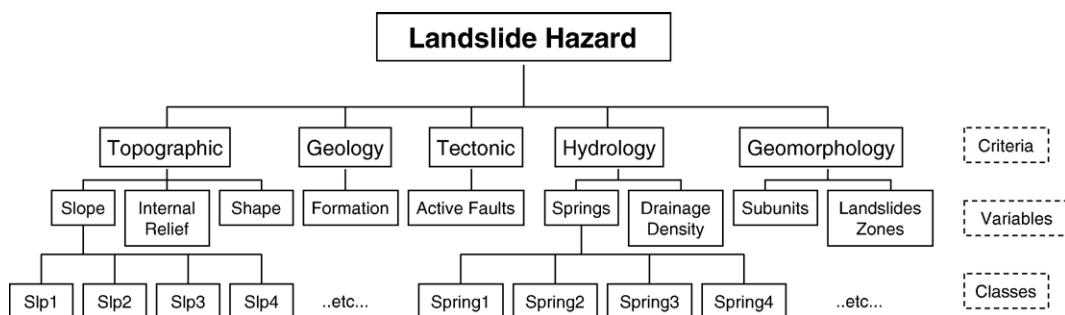


Fig. 5. Components of the heuristic landslide hazard model.

the landslide this information may no longer be reliable. Most of the landslides in the Sierra de Caujerí scarp consist of a large scarp on the upper part, often up to 100 m high, which almost vertically cut the limestone layer of the Yateras formation (Phase2), and the underlying Maguey formation (Phase1). This scarp is actually the back-scarp of multiple landslides, which change from rockslide to debris flows. Around 150 different landslide events have been mapped along the Sierra de Caujerí and Sierra de Mariana scarp (Figs. 2, 3 and 4).

4. Qualitative assessment of landslide hazard

The geomorphological mapping provided in-depth knowledge of the causal factors for landslides in the study area and was used to assess landslide susceptibility. Qualitative weighting, one of the heuristic methods (Soeters and Van Westen, 1996), was selected, given the relative small scale, the available data, and the characteristics of the study area. Besides, the TMU mapping may produce biased results when using a statistical method due to the high spatial correlation between the landslides inventory and some units in the TMU map.

The analysis was carried out in different steps following the decision-support system method, according to the analytic hierarchy process (Saaty, 1980; Saaty and Vargas, 2001). First the various components (causal factors) in the model were selected, and their hierarchical relation determined. Weights then were assigned to these maps, in a standardized way. A combination formula integrated the weights to produce a final map, which was parsed into a number of classes (Bonham-Carter, 1996).

The design of a heuristic landslide hazard model requires thorough analysis of the causative factors and their relationship in the study area. That was done based on the geological and geomorphological interpretation along with the fieldwork campaign. The selection of the model components was organized in a tree-shaped structure (Fig. 5). The upper most general level of the components is called criteria, and consists (in ranked order) of Geomorphology, Topography, Geology, Tectonics, and Hydrology. These criteria were further subdivided into nine variables, specific attributes, such as slope, internal relief and slope shape for Topography. The variables are described in Table 1. The relation of each to landslide occurrence can either be favorable or unfavorable.

Table 1
Variables for the heuristic model

Variable	Origin	Scale	Units	Relation
Slope	From the original DEM using the method of ILWIS software package (ITC, 2001)	Interval	Degrees	Favorable
Internal relief	From the original DEM using the method of ILWIS software package (ITC, 2001)	Ratio	Meters/ hectares	Favorable
Shape	From the original DEM using the method of ILWIS software package (ITC, 2001)	Ratio	N/A	Favorable
Geology	By reclassifying the TMU map	Categorical	N/A	N/A
Faults	Calculating a distance from the fault map and dividing into four classes	Ratio	Meters	Unfavorable
Springs	Calculating a distance from spring points and dividing into four classes	Ratio	Meters	Favorable
Drainage distance	Calculating a distance from the drainage map and dividing into four classes	Ratio	Meters	Favorable
Geomorphological subunits	By reclassifying the TMU map	Categorical	N/A	N/A
Landslides subzones	By reclassifying the TMU map	Categorical	N/A	N/A

See text for explanation (N/A — not applicable).

The variables selected needed to be standardized in order to properly compare them. The values of the variables were converted into a number of classes, depending on the type of variable. Every class received a value between 0 and 100, considering that the value of all classes in one variable need to sum up to 100. Class boundaries for numerical variables were selected from the 25-cumulative percentage intervals of their histogram. The classes of the categorical variables (e.g. geology) were “weighted” according to a ranking method (see below).

Once all the variables were standardized, weights were assigned to the corresponding levels of criteria and variables in three different ways: directly by expert opinion, by pairwise comparison matrix and by ranking. The weight values range between 0 and 1 and need to sum up to 1 among the variables within a criterion and among the criteria. For checking the weight assignment the decision-support system called DEFINITE was used (Janssen and Van Herwijnen, 1994). In the first method the weights of the criteria and variables were assigned directly based on expert opinion and field experience. For the pairwise comparison matrix, each variable (or criterion) is compared to all others in pairs in order to evaluate whether they are equally significant, or whether one of them is somewhat more significant/better than the other for the goal concerned. In the ranking method the criteria and variables are simply ranked according to their importance as landslide controlling factors. The rankings can be considered units on an ordinal scale. Consequently the weights can be found by standardizing the rank order (Voogd, 1983). The values for criteria, variable and classes were tabulated using Microsoft

Excel and a simple summation formula applied to interactively evaluate the effect of the weights on the overall weight of the qualitative landslide hazard.

The three weighting methods gave comparable results, as can be seen from Table 2. For the pairwise comparison matrix method the inconsistency value was 0.08, demonstrating that the weights are sufficiently reliable. The inconsistency parameter measures randomness of the expert judgments, and ranges from 0 to 1. As a conclusion the initial weights assigned by expert opinion were taken for the analysis.

To calculate a final weight for a single pixel the weight of the three components (class value, variable and criterion) was simply multiplied. For example, the slope class “shp4” ($>20.4^\circ$) has a weight of 50, which was multiplied by the weight of the “Slope” variable (0.7) and by the weight of the “Topography” criterion (0.3), so that the final weight was 10.5. Final weights were calculated for each variable and resulted in separate layers, which are generated with the CARIS GIS software package (Universal Systems Ltd, 2000) for the spatial overlay analysis. In this GIS, each class is created in raster format by different options according to the map characteristics: by buffering (e.g. distance to faults), by selecting polygons (e.g. TMU subunits) and by reclassifying pixel values in a raster image (e.g. slope angle values). All weight maps were added into a layer with final weights.

The final weights of the resulting map ranged from 0.5 to 47.1. This map was classified into 10 divisions interactively, during which the relation with existing landslide areas and geomorphological units was evaluated. Although the map gives a good indication of the qualitative landslide hazard in the study area, too many classes might make it difficult to use by decision makers for development planning. Therefore, the hazard map has ten classes, which are grouped into three simplified categories: high, moderate and low (Fig. 6 and Table 3).

The final hazard map was combined with the TMU map-database in order to obtain information about the attributes for each hazard class. Table 3 shows the legend of the final landslide hazard map with statistical information related to the number of landslides and landslide density per class.

Additionally, in the final hazard map the flooding areas were included with two categories: flooding zones (F1) and dam break zones (F2) (Fig. 6 and Table 3). Flooding zones were primarily acquired from a disaster management plan used by the local civil defense authority. The flooding boundaries were corrected by photo-interpretation, DEM analysis and fieldwork. Dam breaks zones were obtained from the dam project reports

Table 2
Weight for criteria and variables for three methods

Components	Direct method	Pairwise matrix	Ranking method	
Topography	0.3	0.224	0.257	
Slope	0.7	0.7	0.7	0.7
Internal relief	0.2	0.2	0.2	0.2
Shape	0.1	0.1	0.1	0.1
Geology	0.2	0.131	0.157	
Formation	1	1	1	1
Tectonic	0.05	0.040	0.065	
Active faults	1	1	1	1
Hydrology	0.05	0.038	0.065	
Springs	0.5	0.5	0.5	0.5
Drainage density	0.5	0.5	0.5	0.5
Geomorphology	0.4	0.566	0.457	
Subunits	0.4	0.4	0.4	0.4
Landslides zones	0.6	0.6	0.6	0.6
Total for criteria	1	0.999	1.001	

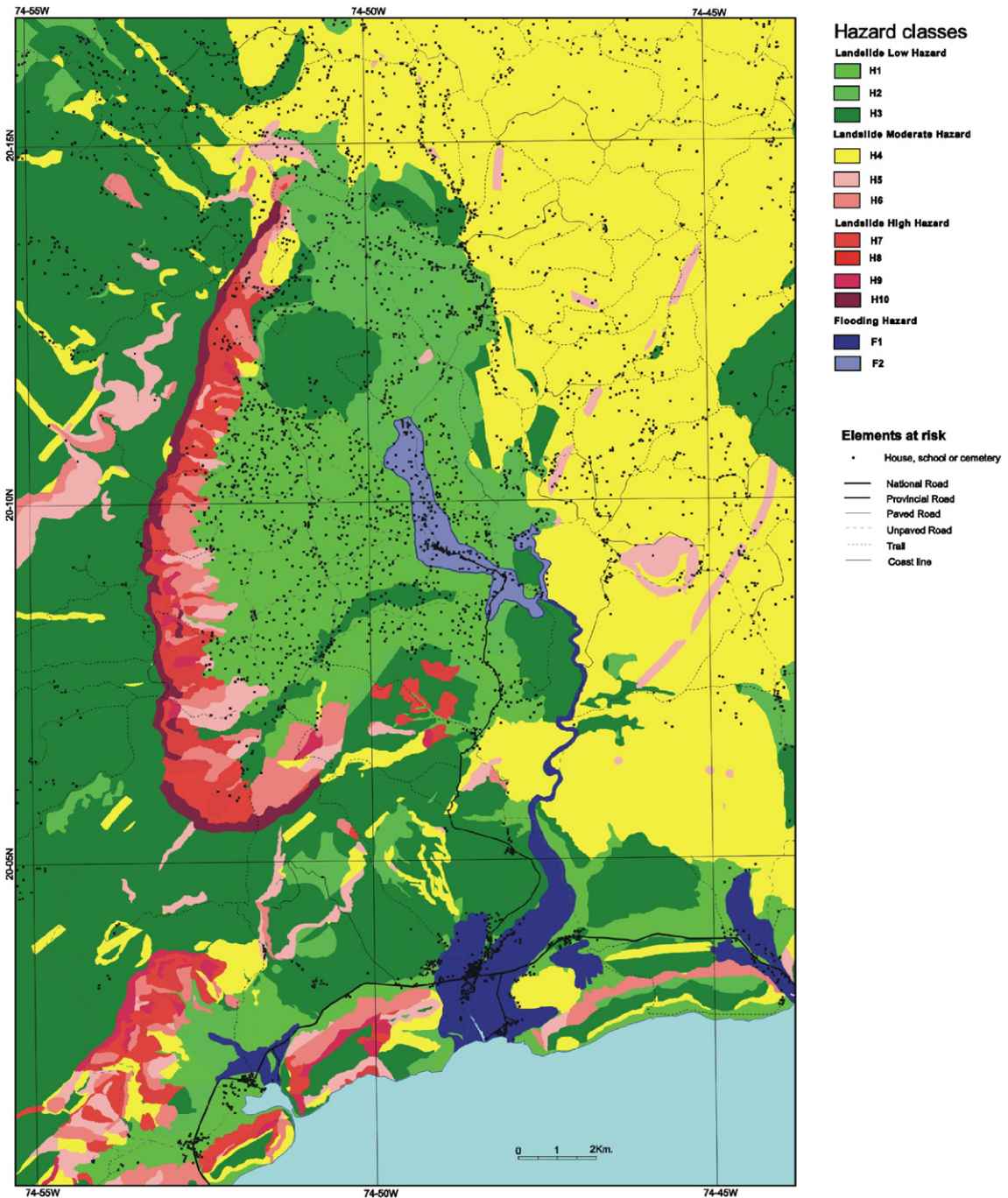


Fig. 6. Landslide hazard map. San Antonio del Sur, Guantánamo, Cuba. See Table 3 for explanation of the legend.

made by the Institute of Water Resources for Guantánamo province. The two areas mapped are related to Pozo Azul and Palmarito dams. Dam location and names appear in Fig. 2. More detail information about the flooding zones was available, but could not be displayed at 1:50,000 scale.

5. Qualitative assessment of landslide risk

Too little information was available to carry out a more sophisticated landslide risk assessment. In particular, there were not enough data on the probability of landslides of different magnitudes to make a (semi) quantitative risk

Table 3

Characterization of the 10 landslide hazard classes and 2 flooding hazard classes (see Fig. 6)

Hazard	Overall class	Hazard class	Weight range	Area (ha)	Number of TMU units	Number of landslides	Area of landslides (ha)	Landslide density (%)	General hazard description	
Landslides	Low	H1	0.50–5.16	8669	88	0	0	0	No landslides expected. Areas can be corridors for mudflows or other intensive mass wasting processes. In some parts small landslides can happen in extreme conditions. The areas are suitable for development projects. Moderate to high possibility of landslides occurrence during intensive or prolonged rainfall. These areas contain most of the existing landslide zones. Most of the landslide materials are unconsolidated and susceptible to being reactivated in smaller proportions. More studies are required for development of the area. Land use changes should be previously studied in relation to landslide hazard problem. High to very high landslide hazard areas. A high possibility of landslide occurrence during rainy conditions. No development is recommended in these areas. Possible relocation of land for agricultural use. Highly recommended re-allocation of existing population in these areas.	
		H2	5.17–9.82	4176	40	0	0	0		
		H3	9.83–14.48	18,107	125	8	8	210		1.1
	Moderate	H4	14.49–19.14	18,361	94	22	22	338		1.8
		H5	19.15–23.80	2013	85	46	46	901		44.7
		H6	23.81–28.46	1,702	87	79	79	1,428		83.8
	High	H7	28.47–33.12	969	77	76	76	963		99.3
		H8	33.13–37.78	719	59	59	59	715		99.5
		H9	37.79–42.44	291	36	36	36	289		99.4
		H10	42.45–47.10	439	24	24	24	438		99.8
Floods		F1	N/A	1325	15	0	0	0	Flooding areas up to 5 years return period taken from local civil defense authority and updated yearly. Appropriate warning system needs to be maintained. The area could be used for seasonal agricultural products. Land-use planning should consider flooding hazard limits to re-allocated existing infrastructure and avoid new developments. Dam break flood limit taken from dam project report. Engineering conditions of the dam should continuously be checked. The area could be used for agricultural products. Land-use planning should consider this hazard limit to re-allocated existing infrastructure and avoid new developments.	
		F2	N/A	503	6	0	0	0		

assessment. Therefore only a basic qualitative analysis was carried out through the combination of the landslide hazard map with basic elements at risk. During the fieldwork, information was collected on buildings and roads. As the study area is a rural environment, most of the buildings are isolated farmhouses; a number of small schools and medical centers also were identified. Most roads are unpaved country roads, except for the main road in the south of the study area, which runs along the coast, mostly on the land-side of the coastal hills. The roads and buildings are indicated in Fig. 6. No attempt was made to evaluate the potential losses of crops. In the study area there are a few small settlements, of which San Antonio

del Sur is the largest. Other villages and hamlets are Puriales de Caujerí, Baitiquirí, Macambo, Guaibanó, and El Naranjo (see names in Fig. 2).

Most of the 3317 buildings in the study area are made of wood over a concrete base, and few are of masonry only or of reinforced concrete cement (RCC), which are nearly all found in the settlements. There are 88 small schools scattered over the area, 6 medical centers and 4 small cemeteries. Building density is highest in the central-north part of the Caujerí depression, where many buildings are at risk in case a large landslide originates from the Caujerí scarp. To analyze the qualitative risk level of the buildings, GIS overlay was calculated between the building map and

the hazard map. The result is shown in Table 4. Most buildings and all of the small schools are located in low and moderate landslide hazard zones. No buildings are currently in the highest hazard zones. A similar analysis was made for the road network (see Table 4). The provincial and national roads do not cross the high hazard areas, although quite a few roads are in the moderate hazard classes. To refine these results in the future more data related to the elements at risk should be collected, including population distribution, and the replacement value of buildings and roads, as well as the value of different agricultural crops.

6. Discussion and conclusions

Detailed geomorphological mapping provides information on the site-specific conditions under which different landslide types occur in different parts of the study area. Landslides are concentrated along the Caujerí scarp, but also in the coastal hills and in the northern part of the Baitiquirí area. There, the landslides have different characteristics and causative factors. Subdivision of the terrain into 603 terrain mapping units, individual homogeneous polygons, allowed for a more detailed characterization of the terrain than would be possible through conventional map-overlay of main factor maps. The boundaries of different landslide parts were surveyed by photo-interpretation, and landslides were described in the field from a detailed checklist, where information was collected related to landslide type, subtype, relative age, and depth.

This data set enable us to generate a heuristic model, using multicriteria analysis, which was successful in classifying the area into different hazard classes, which can be displayed either in 10 more detailed or 3 generalized

classes, depending on the user's map needs. Improvements in the method could be made if different weight maps were produced for different landslide types. However, since the geomorphological units are one of the main variables in the heuristic analysis, this could be partly taken into account, by assigning weights to each individual unit.

Overall landslide qualitative hazard can be considered rather low, with the exception of a number of specific areas, such as the Caujeri scarp, and the area directly below. However, due to the absence of a sufficiently long landslide record, it was not possible to indicate probabilities assigned to the 10 classes. Historical landslide information is not available, except for a few isolated landslides. It is known that large landslide can happen along the Sierra de Caujeri, similar to the failure that occurred in 1963 during the passage of a hurricane. The situation in the study area can be considered as representative for the whole of Cuba, where due to the lack of a landslide inventory, the knowledge about landslide causative factors and mechanisms is still limited.

Recently, however, the National Civil Defense and the Ministry of Science, Technology and Environment have decided to establish a system for landslide risk assessment in the Cuban Archipelago. The system will include the design and implementation of a national landslide inventory database and landslide risk-assessment procedures at different disaster management levels (Castellanos and Van Westen, 2005).

An important component of this system will be the involvement of local staff of the Civil Defense at the 169 municipal centers, including San Antonio del Sur. A simple landslide reporting form has been designed, and workshops will be conducted to train the staff and make them aware of the procedure. Once the local officers report a landslide, a landslide expert from the central office will

Table 4
The number of buildings and length of roads per hazard class

Hazard classes	Buildings (nr)	Houses (nr)	Schools (nr)	Cemeteries	National roads (km)	Provincial roads (km)	Paved roads (km)	Unpaved roads (km)
H1	1370	1338	29	3	33.3	27.9	29.4	151.4
H2	381	367	13	1	2.4	0	17.6	48.9
H3	588	570	18	0	5.6	20.7	15.7	132.4
H4	947	919	28	0	0.1	1.2	7.4	120.6
H5	69	68	0	1	0.1	0	0	16.6
H6	36	36	0	0	0.6	0	0.9	5.8
H7	30	29	1	0	0	0	0	7.9
H8	14	14	0	0	0	0	0.7	0.8
H9	0	0	0	0	0	0	0	1.1
H10	1	1	0	0	0	0	0	0
Total	3436	3342	89	5	42.1	49.8	71.6	484.6
Actual nr.	3409	3317	88	4				

The small difference between the total and the actual number is due to processing errors in the rasterization procedure.

visit the site and complete the questionnaire in more detail. Such a system for landslide data collection might be less effective in other countries, due to insufficient reporting staff at the local level. In Cuba, however, the Civil Defense is well organized and very effective as reflected in a comparison of disaster-related casualties numbers in Cuba with those of neighboring countries such as Haiti or the Dominican Republic (Thompson and Gaviria, 2004).

Acknowledgements

We thank Koert Sijmons for his assistance in generating the maps. The research was coordinated with the National Science and Technological Innovation Program for Civil Defense (PNCIT) and the National Headquarters of the Civil Defense (EMNDC) in Cuba. The Institute of Geology and Paleontology (IGP) has been carrying out this project since January 2004 for four study areas with duration of 3 years. This work is a component of the ITC SLARIM research project: Strengthening Local Authorities in Risk Management. Finally, many thanks to Dr. Richard Pike and Dr. Mauro Cardinali for their constructive comments on the manuscript.

References

- Aleotti, P., Chowdhury, R., 1999. Landslide hazard assessment: summary review and new perspectives. *Bulletin of Engineering Geology and Environment* 58, 21–44.
- Barredo, J., Benavides, A., Hervas, J., van Westen, C.J., 2000. Comparing heuristic landslide hazard assessment techniques using GIS in the Tirajana basin, Gran Canaria Island, Spain. *International Journal of Applied Earth Observation and Geoinformation* 2, 9–23.
- Bonham-Carter, G.F., 1996. *Geographic Information Systems for Geoscientists: Modeling with GIS*. Pergamon, Elsevier, Amsterdam. 398 pp.
- Castellanos, E., Van Westen, C.J., 2005. Development of a system for landslide risk assessment for Cuba. *Proceedings International Conference on Landslide Risk Management*, May 31–June 3, 2005, Vancouver. 764 pp.
- Chang, J.L., Suarez, V., 1998. Fuentes magnéticas anómalas profundas y su implicación en el modelo tectónico de Cuba oriental. *Memoria del tercer congreso cubano de geología y minería (Sociedad Cubana de Geología)*, vol. 1, pp. 169–172.
- Franco, G. (Ed.), 1992. *Léxico Estratigráfico de Cuba*. Instituto de Geología y Paleontología, La Habana. 410 pp.
- Guzzetti, F., Carrara, A., Cardinali, M., Reichenbach, P., 1999. Landslide hazard evaluation: a review of current techniques and their application in a multi-scale study, Central Italy. *Geomorphology* 31, 181–216.
- ITC, 2001. ILWIS 3.0 software package. User's Guide. ITC, Enschede, Netherlands. 520 pp. <http://www.itc.nl/ilwis/default.asp>.
- Iturralde-Vinent, M.A. (Ed.), 1996. Cuban Ophiolites and Volcanic Arcs. Project 364: Geological Correlation of Ophiolites and Volcanic Arcs Terranes in the Circum-Caribbean Realm. *Contribution*, vol. 1. 256 pp.
- Janssen, R., Van Herwijnen, M., 1994. Multiobjective decision support for environmental management. *DEFINITE Decisions on an FINITE Set of Alternatives*. Klumer Dordrecht. 132 pp.
- Latelín, O., 1997. Berücksichtigung der Massenbewegungsgefahren bei raumwirksamen Tätigkeiten. *Empfehlungen 1997*. Swiss Federal Office for the Environment (FOEN). <http://www.bwg.admin.ch/themen/natur/e/index.htm>.
- Lee, E.M., Jones, D.K.C., 2004. *Landslide Risk Assessment*. Thomas Telford, London. 454 pp.
- Magaz, A., Hernández, J. R., Díaz, J.L., Venero, A., Pérez, F., Blanco, P., Fundora, M., Cruz, C., 1991. El complejo de formas del relieve gravitacional en la franja costera Baitiquiri-Punta Maisí, Provincia de Guantánamo, Cuba. In: *Colectivo de Autores (Editor), Morfotectónica de Cuba Oriental*. Editorial Academia, La Habana, pp. 28–43.
- Meijerink, A.M.J., 1988. Data acquisition and data capture through terrain mapping units. *ITC Journal* 1988 1, 23–44.
- Millán, G., Somin, M., 1985. Contribución al conocimiento geológico de las metamorfitas del Escambray y Purial: reportes de investigación, vol. 2. *Academia de Ciencias de Cuba*, pp. 1–74.
- Nagy, E., Brezsnýánszky, K., Brito, A., Coutín, D., Formell, F., Franco, G.L., Gyarmaty, P., Jakus, P., Radocz, Gy., 1983. Contribución a la Geología de Cuba Oriental. *Editorial Científico-Técnica*, La Habana. 273 pp.
- Núñez, A., Sánchez, R., Cordovez, R., Reborido, J., Rosales, C., Nicolaiev, A., Metetskoy, F., Skorina, P., Demidov, V., 1981. Informe geológico sobre los trabajos de levantamiento, búsqueda a escala 1:100 000 y los resultados de los trabajos búsqueda a escala 1:50 000 Y 1:25 000 ejecutados en la parte este de la provincia de Guantánamo, ONRM. MINBAS, La Habana.
- Saaty, T.L., 1980. *The Analytic Hierarchy Process*. McGraw Hill, New York.
- Saaty, T.L., Vargas, L.G., 2001. *Models, Methods, Concepts, and Applications of the Analytic Hierarchy Process*. Kluwer Dordrecht. 333 pp.
- Soeters, R., Van Westen, C.J., 1996. Slope instability. Recognition, analysis and zonation. In: Turner, A.K., Schuster, R.L. (Eds.), *Landslide: Investigations and Mitigation*. Special Report, vol. 247. Transportation Research Board, National Research Council, National Academy Press, Washington, D.C., pp. 129–177.
- Thompson, M., Gaviria, I., 2004. Cuba, weathering the storm. Lessons in risk reduction from Cuba. *Oxfam America Report*. Website: www.oxfamamerica.org/cuba. 65 pp.
- Trusov, I., 1989. Sección Clima VI.3.4. 37 Eventos notables. 37a Flora. In: *Instituto de Geografía Tropical (Editor)*, *Nuevo Atlas Nacional de Cuba*. Instituto Geográfico Nacional de España, La Habana, Cuba.
- Universal Systems, Ltd, 2000. CARIS GEMM software package. *CARIS User's Manual*, Fredericton, Canada. <http://www.caris.com>.
- Van Westen, C.J., Soeters, R., Sijmons, K., 2000. Digital Geomorphological landslide hazard mapping of the Alpage area, Italy. *International Journal of Applied Earth Observation and Geoinformation* 2, 51–59.
- Van Westen, C.J., Rengers, N., Soeters, R., 2003. Use of geomorphological information in indirect landslide susceptibility assessment. *Natural Hazards* 30, 399–419.
- Voogd, H., 1983. *Multicriteria Evaluation for Urban and Regional Planning*. Pion, London. 367 pp.